Supplementary Information (SI) for Polymer Chemistry.
This journal is © The Royal Society of Chemistry 2025

Photo-curable resins based on poly(globalide) for 3D printing of resorbable scaffolds: synthesis, crosslinking and post-functionalization

Laura Oliveira Rebouças, Isabela Lima Autran Dourado, Giovanne Delechiave, Denisse Esther Mallaupoma Camarena, Sandra Van Vlierberghe, Luiz Henrique Catalani

SUPPORTING INFORMATION

1. ^{1}H NMR for PGl-DG and PGl-DG-AC with integration values

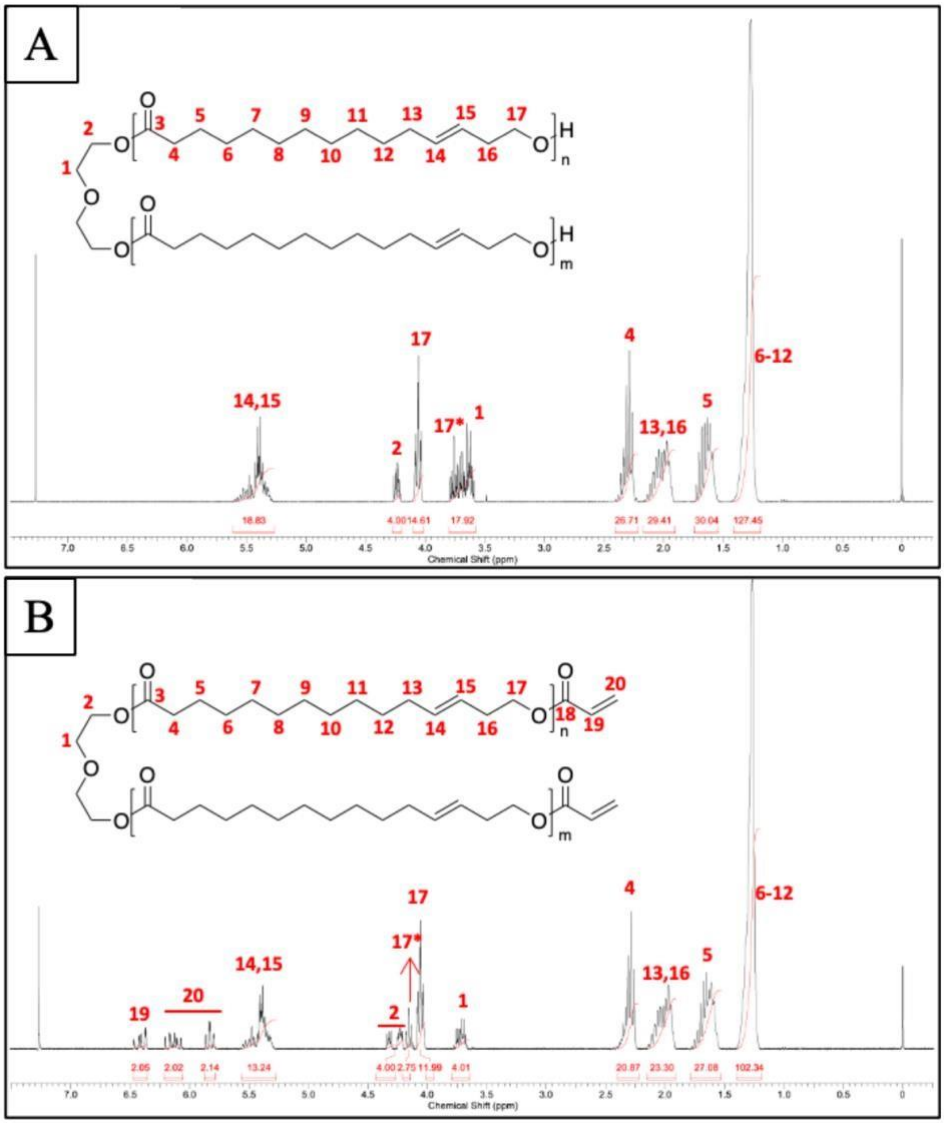

Figure S1. ^{1}H-NMR spectra for (A) PGl-DG and (B) PGl-DG-AC with integration values.

2. ^{13}C-NMR for PGl-DG and PGl-DG-AC

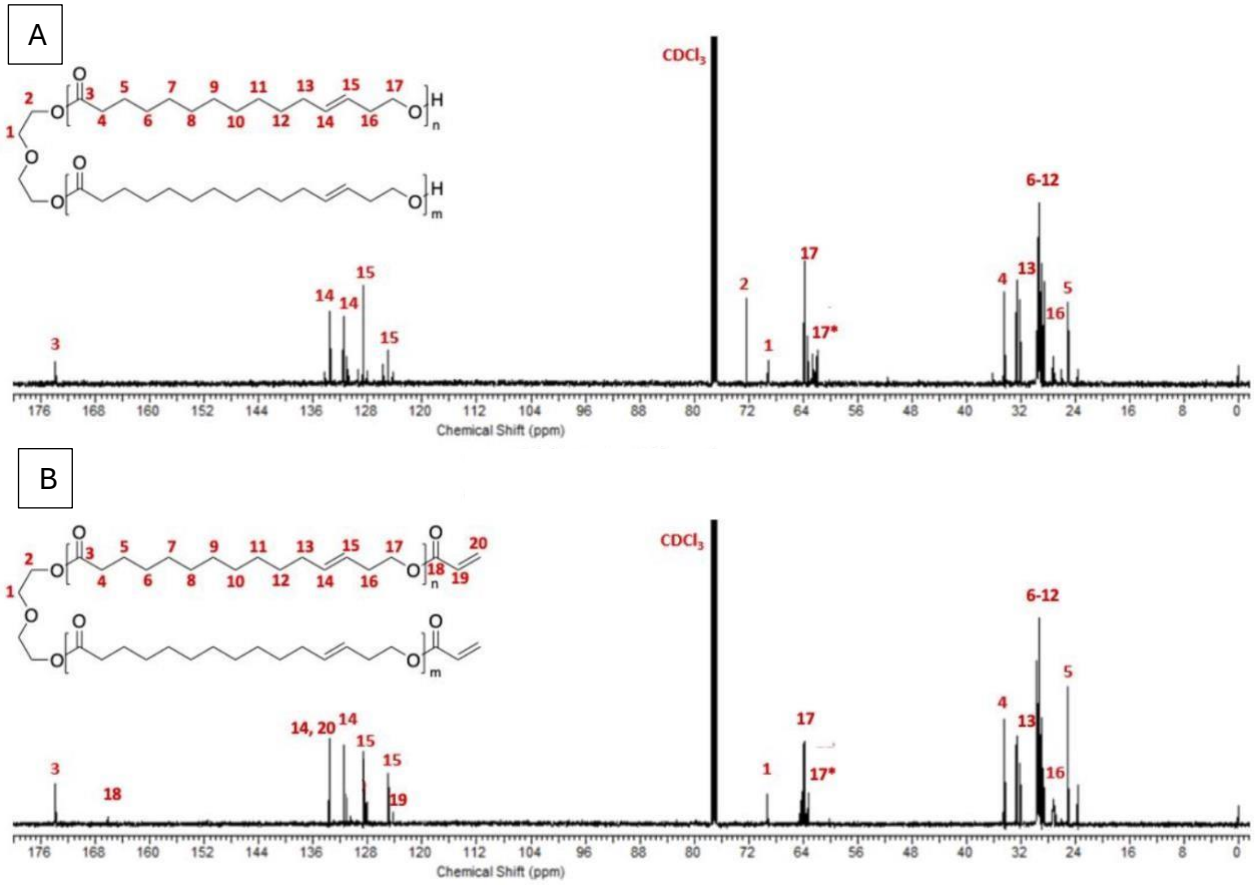

Figure S2. ^{13}C-NMR spectra for (A) PGl-DG and (B) PGl-DG-AC.

3. Gel Permeation Chromatography (GPC)

Table S1. Molecular weight distribution obtained for homopolymers of globalide initiated by diethylene glycol.

m_{GL} / m_{DG}	$\bar{M}_w$ (kg mol^{-1})	$\bar{M}_n$ (kg mol^{-1})	PDI
650	3.2	2.5	1.3
520	4.5	3.1	1.4
390	5.4	4.2	1.3
265	6.0	4.5	1.3
130	8.1	5.7	1.4
65	11.9	7.6	1.6

4. Relation between the degree of substitution and the excess of acryloyl chloride

Table S2. Stoichiometric ratio of hydroxyl groups and DS achieved.

Ratio*	DS expected (%)	DS achieved (%)
1:1.2	100	19
1:6	100	100
1:8	100	100

*ratio between -OH groups from PGl-DG and acryloyl chloride moieties

The degree of substitution was calculated by ^{1}H NMR integration for signals corresponding to the methylene groups from diethylene glycol (split in 4.24 ppm and 4.35 ppm) and to the olefinic signals from acrylic groups in the region of 5.3—6.6 ppm.

$$degree\ of\ substituion\ (\%) = \frac{\frac{(I_{\partial 5.8} + I_{\partial 6.1} + I_{\partial 6.4})}{3}}{\frac{(I_{4.2} + I_{4.3})}{2}} 100\%$$

5. MALDI-TOF of PGl-DG and PGl-DG-AC

MALDI-TOF was employed to confirm the chemical structure of PGl-DG and PGl-DG-AC. As one can see in Figure S3, the mass spectra for both materials show underrated m/z values compared to the molecular weight obtained by GPC. The spacing between peaks for PGl-DG and PGl-DG-AC reveals an addition of m/z 238.4 for each adduct, relating to the repetitive globalide residue units. The mass spectra confirms that e-ROP was successfully initiate by EG (A) but there is also a less representative family of macromolecules initiated by water (B) probably from the inherent layer of water present surrounding the surface of the enzyme (CAL-B).

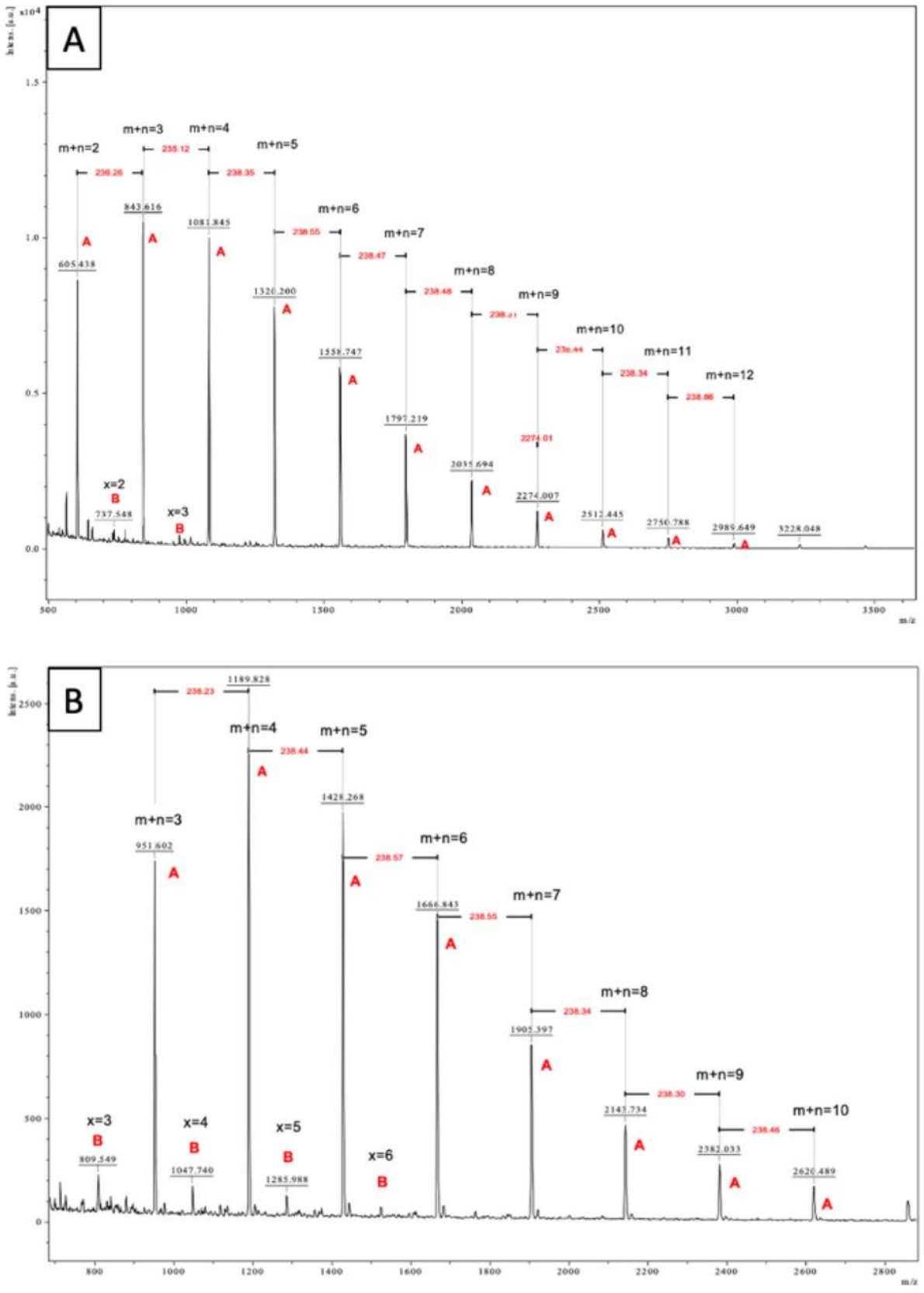

Figure S3. MALDI-TOF spectra for A) PGl-DG and B) PGl-DG-AC. “A” represents family of macromolecules that were initiated by diethylene glycol whereas “B” represents the family initiated by water (“m+n” and “x” represent the total amount of globalide residues in each peak).

The peaks A and B in Figure 3S-A are, respectively, representative of the following structures:

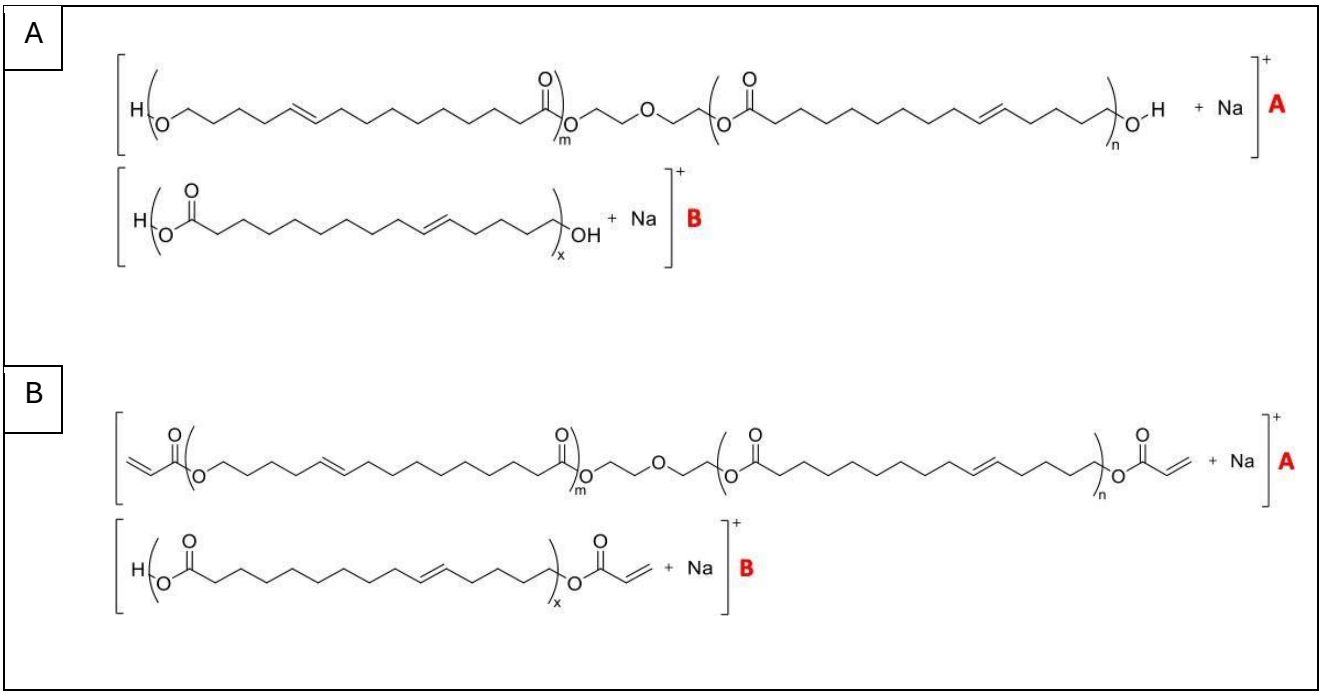

Figure S4: (A) schematic representation of polymer structures attributed to peaks A and B in Fig. 3S-A; **(B)** schematic representation of polymer structures attributed to peaks A and B in Fig. 3S-B.

The values of m+n and x in the Figure S3 represent the total amount of globalide residues per molecule in each peak. Since acrylic modification occurs only in hydroxyl groups, macromolecules from the B family have one acrylic group per chain, whereas the ones from the A family have two acrylates in each chain.

6. Thermal Analysis for PGl-DG and PGl-DG-AC

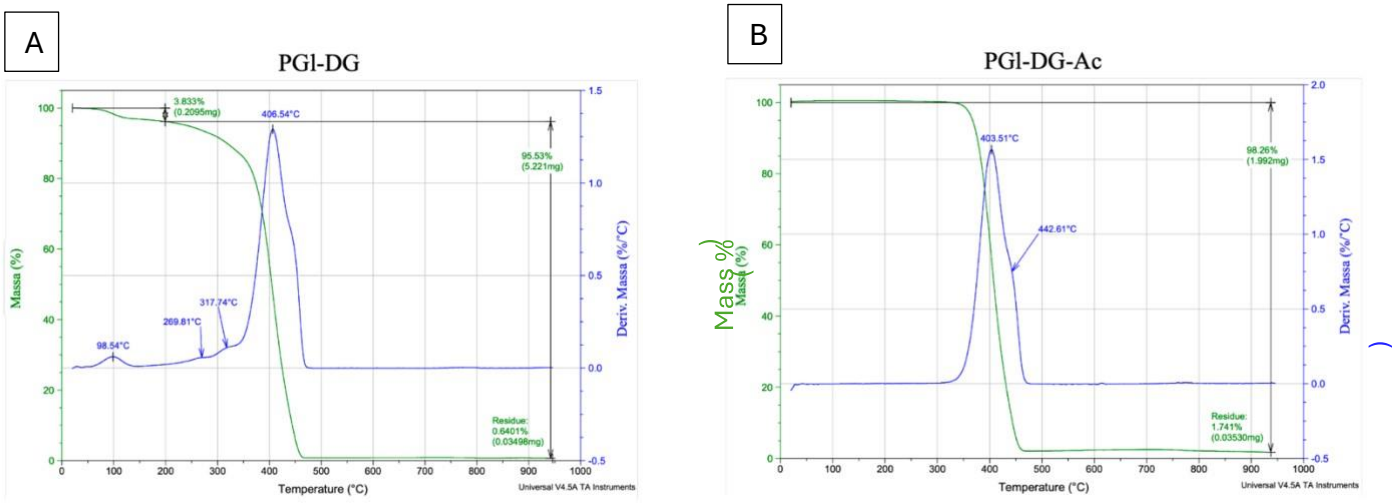

Figure S5. TGA thermograms PGl-DG (A) and PGl-DG-AC (B).

7. X-Ray Analysis

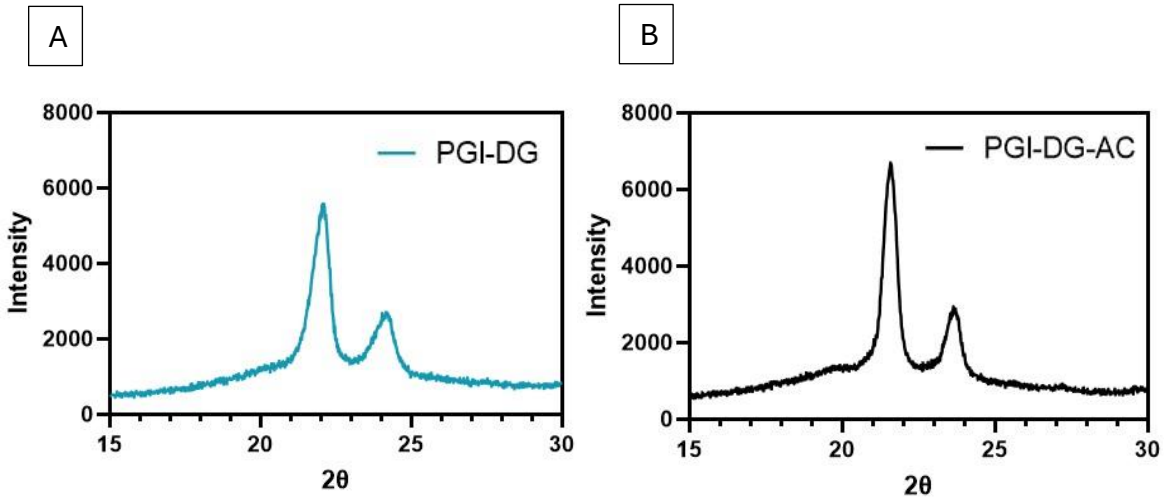

Figure S6. WAXD scattering spectra for semi-crystalline PGl-DG (A) and PGl-DG-AC (B).

8. Weight fractions of PGl-DG-AC formulations

Table S3. Weight fractions of the different formulations that were used.

	P_	P_NIPAM	P_NVP	P_PEGDA	P_DECDA
Polymer (PGl-DG-AC) (mg)	233.3	233.3	233.3	233.3	233.3
Photo-initiator (BAPO) (mg)	18	18	18	18	18
Solvent (DCE) (mL)	1	1	1	1	1
Unsaturated monomer (mg)	-	135.3	133.3	233.3	135.3

9. DSC of the photo-crosslinked films

To assess whether the films kept the crystalline domains that were present in the polymer before crosslinking, the DSC second heating curves for each films was analyzed. It is worth to say that each film presented a different degradation temperature (T_d), thereby the DSC analyses proceed during heating from -20ºC until (T_d-20) ºC

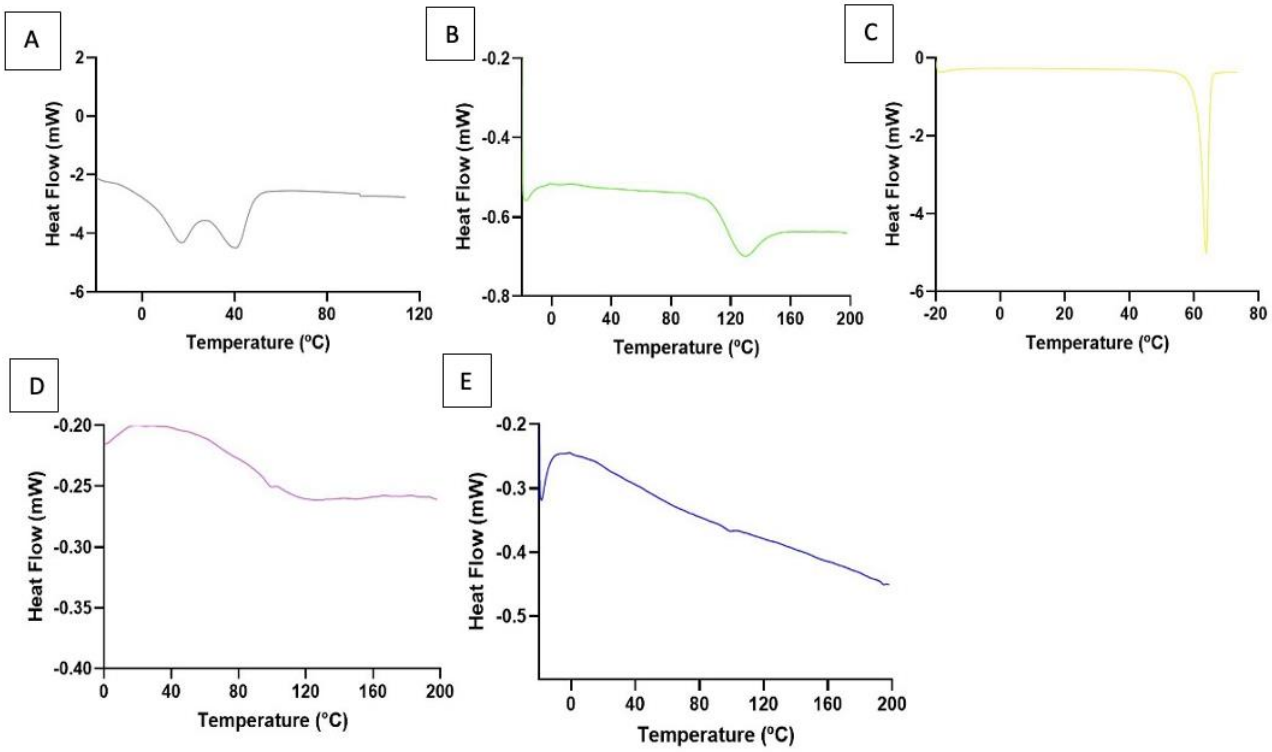

Figure S7. DSC curves (second heating scans) of (A) P_, (B) P_NVP, (C) P_NIPAM; (D) P_PEGDA; (E) P_DECDA

9. Rheology

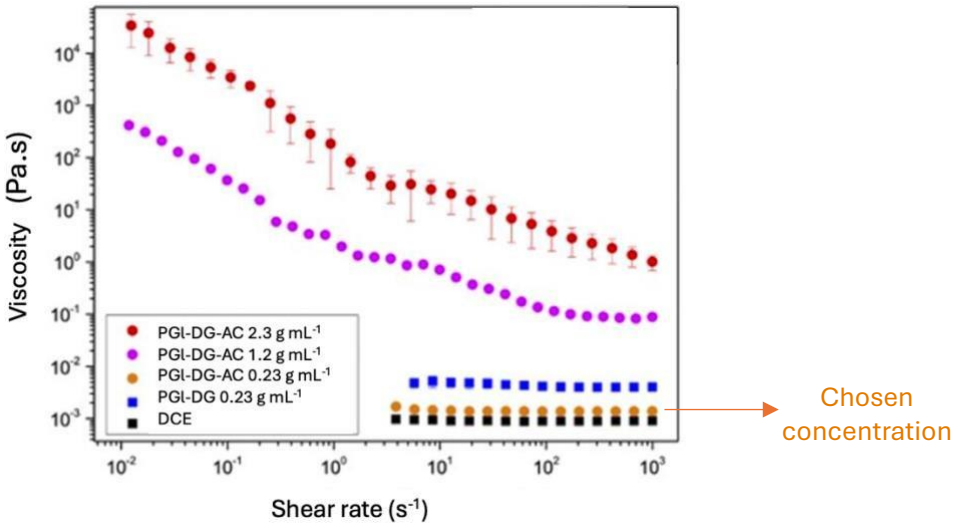

Figure S8. Flow curves for PGl-DG and PGl-DG-AC in different concentrations.

10. Modifications in the 3D printer

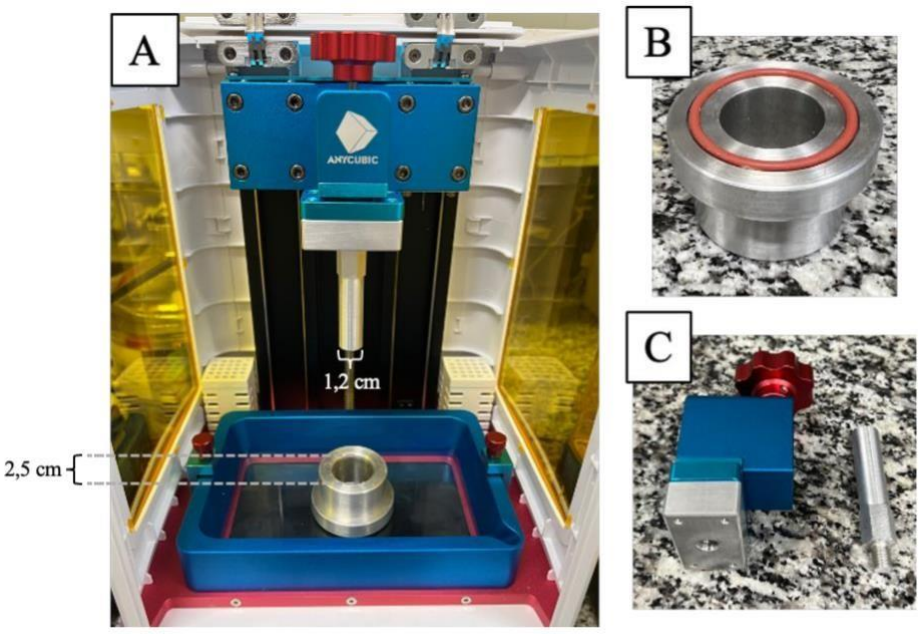

Figure S9. Pictures of the customized LCD-based Photon S from Anycubic. (A) 3D printer without the lid with new dimensions of vat and build platform; (B) bottom of new vat with a rubber ring; (C) new small build platform in detail.

11. Working curve for the resin of PGl-DG-AC + PEGDA

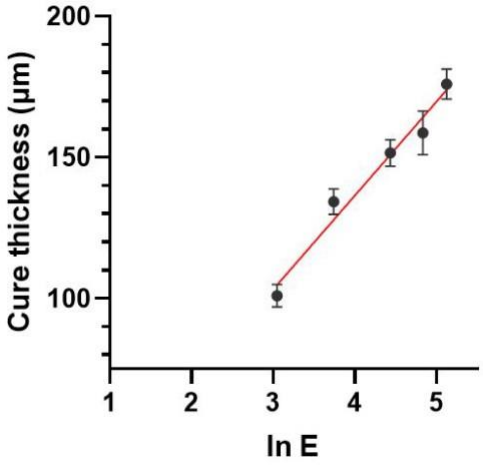

$C_d = D_p \ln E - Dp \ln E_c$

$C_d = 33.3 \ln E - 0.1016$ (linear regression)

in which $D_p = 33.3$ µm

and $\ln E_c = 0.1016/Dp \Rightarrow E_c \approx 1$ mJ cm^{-2}

Figure S10: Jacob's working curve for the formulation containing PGl-DG-AC and PEGDA.

12. 3D printing of simple constructs

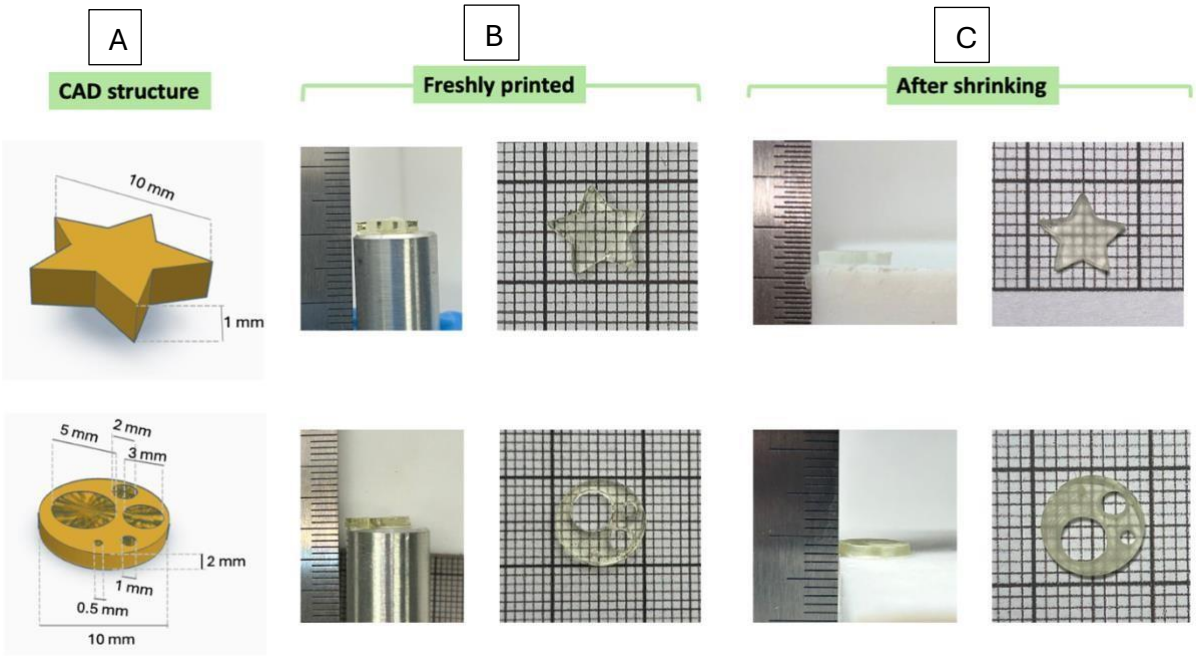

Figure S11. (A) CAD designs with pre-defined dimensions; (B) pictures of freshly printed parts; (C) pictures of printed parts after shrinking (all parts were left to dry for 72h). The same formulation containing PGl-DG-AC and PEGDA was used in all cases.

The disc with internal hollows was designed to assess the X-Y resolution. Under these conditions, the resolution limit ranges between 0.5 and 1 mm. After crosslinking, the diameter of the smallest hollow is approximately 1 mm. Adding a photo-absorber could help prevent unwanted crosslinking within the hollows.